NEURAL REGENERATION RESEARCH
Volume 8, Issue 36, December 2013

www.nrronline.org

doi:10.3969/j.issn.1673-5374.2013.36.003 [http://www.nrronline.org; http://www.sjzsyj.org]
Lin EJ, Long HQ, Li GS, Lei WL. Does diffusion tensor data reflect pathological changes in the spinal cord with chronic injury? Neural Regen Res. 2013;8(36):3382-3390.

Does diffusion tensor data reflect pathological changes in the spinal cord with chronic injury?*****

Erjian Lin[1], Houqing Long[2], Guangsheng Li[3], Wanlong Lei[4]

1 *Department of Radiology, the Eastern Hospital of the First Affiliated Hospital, Sun Yat-sen University, Guangzhou 510700, Guangdong Province, China*
2 *Department of Spinal Surgery, Huangpu Branch, First Affiliated Hospital of Sun Yat-sen University, Guangzhou 510700, Guangdong Province, China*
3 *Department of Orthopedics, Affiliated Hospital of Guangdong Medical College, Zhanjiang 524001, Guangdong Province, China*
4 *Department of Human Anatomy and Histoembryology, Zhongshan School of Medicine, Sun Yat-sen University, Guangzhou 510086, Guangdong Province, China*

Research Highlights

(1) This study was innovative as it was the first to use a novel spongy polyurethane material, which expanded over time after implantation in the rat $C_{3–5}$ epidural space. This method perfectly lates the process of chronic compression.
(2) The present study used a 47 mm coil for magnetic resonance imaging that has rarely been used previously, but could ensure the accuracy of signal-to-noise ratio and data measurement. 1.5 T magnetic resonance imaging was used, which is closer to the clinical settings.
(3) This study revealed fractional anisotropy and average diffusion coefficient in cervical spinal cord compression, which correctly reflected the alterations in the number of neurons in the anterior horn of gray matter of the spinal cord and the density of nerve fibers in the white matter. These findings suggested that image data can be employed to predict pathological changes in the spinal cord and to conduct early diagnosis.

Abstract

Magnetic resonance diffusion tensor imaging has been shown to quantitatively measure the early pathological changes in chronic cervical spondylotic myelopathy. In this study, a novel spongy polyurethane material was implanted in the rat $C_{3–5}$ epidural space to establish a rat model of chronic cervical spondylotic myelopathy. Diffusion tensor data were used to predict pathological changes. Results revealed that the fractional anisotropy value gradually decreased at 4, 24, and 72 hours and 1 week after injury in rat spinal cord, showing a time-dependent manner. Average diffusion coefficient increased at 72 hours and 1 week after implantation. Hematoxylin-eosin staining and Luxol-fast-blue staining exhibited that the number of neurons in the anterior horn of the spinal cord gray matter and the nerve fiber density of the white matter gradually reduced with prolonged compression time. Neuronal loss was most significant at 1 week after injury. Results verified that the fractional anisotropy value and average diffusion coefficient reflected the degree of pathological change in the site of compression in rat models at various time points after chronic spinal cord compression injury, which potentially has a reference value in the early diagnosis of chronic cervical spondylotic myelopathy.

Key Words

neural regeneration; magnetic resonance; cervical spinal cord compression; pathology; diffusion tensor imaging; cervical cord; cervical myelopathy; neurofilament; grants-supported paper; neuroregeneration

Erjian Lin, Master, Technician-in-charge.

Corresponding author: Houqing Long, M.D., Associate professor, Associate chief physician, Master's supervisor, Department of Spinal Surgery, Huangpu Branch, First Affiliated Hospital of Sun Yat-sen University, Guangzhou 510700, Guangdong Province, China, houqinglong@163.com. Wanlong Lei, M.D., Professor, Doctoral supervisor, Department of Human Anatomy and Histoembryology, Zhongshan School of Medicine, Sun Yat-sen University, Guangzhou 510086, Guangdong Province, China, leiwl@mail.sysu.edu.cn.

Received: 2013-08-06
Accepted: 2013-11-17
(N20120910002)

Acknowledgments: We are very grateful to Mao LJ from Department of Imaging and Liang YY from the Department of Neurology, First Affiliated Hospital of Sun Yat-sen University, China for data processing and statistical analysis.

Funding: This study was supported by the Natural Science Foundation of Guangdong Province of China, No. S2011010004843; the National Natural Science Foundation of China, No. 30770679, 31070941, 30570572; the Major Basic Research of Ministry of Science and Technology of China (973 Project), No. 2010CB530004.

Author contributions: Lin EJ provided and integrated data and wrote the manuscript. Long HQ served as a principle investigator, obtained the funding, and analyzed the data. Li GS prepared pathological specimens, participated in statistical treatment, and provided technical and data support. Lei WL served as a principle investigator, obtained the funding, and was in charge of study concept and design. All authors approved the final version of the paper.

Conflicts of interest: None declared.

Ethical approval: This study was approved by the Animal Medical Ethics Committee, First Affiliated Hospital of Sun Yat-sen University, China.

Author statements: The manuscript is original, has not been submitted to or is not under consideration by another publication, has not been previously published in any language or any form, including electronic, and contains no disclosure of confidential information or authorship/patent application/funding source disputations.

INTRODUCTION

Chronic cervical spondylotic myelopathy refers to chronic spinal cord compression injury induced by spinal canal stenosis, ossification of the posterior longitudinal ligament, ligamentum flavum hypertrophy, destabilization of cervical vertebra and intraspinal tumor, resulting in loss of sensation and motor function[1]. During the onset of cervical spondylotic myelopathy, spinal cord white matter fibers are compressed and connective tissue begin to proliferate, thus affecting fiber arrangement. Diffusion tensor imaging detects injury to white matter fibers. It found that the degree of injury is evaluated by calculating fractional anisotropy. At present, the surgery was considered to be an effective therapeutic method for cervical spondylotic myelopathy. However, after injury, some patients still experience spinal cord dysfunction, even aggravation. In addition, nerve symptoms appearing in the clinic are not consistent with the degree of spinal cord compression. Thus, the choice of surgery and prognostic evaluation is difficult and controversial[2-3]. This study explored the feasibility of using data obtained using diffusion tensor magnetic resonance imaging (DT-MRI) to investigate pathological changes.

MRI is an ideal non-invasive method for examining cervical spondylotic myelopathy. Numerous studies have investigated the examination and pathomechanism of cervical spondylotic myelopathy using imaging techniques[4-8]. Conventional MRI images revealed alterations in the anatomical form of the cervical cord and its surrounding tissues, such as intervertebral disc protrusion and hyperostosis. Injury to the cervical cord was mainly examined by observing whether the spinal cord was compressed using MRI images and by determining the degree of compression. When cervical cord injury was very severe, cervical cord degeneration or necrosis can be determined by changes in T1-weighted image (T1WI) or T2-weighted image (T2WI) signals. However, the changes in MRI images were not identical to clinical symptoms in some cases. Moreover, MRI images cannot reveal the pathological changes in neurons and fiber bundles.

Recent studies demonstrated that DT-MRI can be used to measure fractional anisotropy and average diffusion coefficient under pathological conditions, as the diffusion probability of hydrone is different in the living body in various directions. Thus, the functional status of hydrone diffusion exchange in each tissue was determined. In the early stages of cervical spondylotic myelopathy, DT-MRI showed that the alterations in fractional anisotropy and average diffusion coefficient appeared earlier than in MRI images[9-11]. Thus, DT-MRI has the potential to quantitatively measure pathological changes in the spinal cord. Presently, MRI alone cannot precisely judge the characterization and degree of pathological changes in the central nervous system. Simultaneously, it is difficult to perform basic research concerning pathophysiological mechanisms only dependent on clinical cases. Therefore, only by establishing standard repeatable animal models that can simulate the natural course of chronic spinal compression and provide evidence for studying the mechanisms underlying spinal cord injury can we then explore effective intervention methods. Previous studies established animal models of cervical spondylotic myelopathy mainly using balloon, screw and dynamic compression of spinal cord[12-15]. However, acute or subacute spinal cord injury can be induced during model establishment using these methods, repeatability was poor, and the death rate was high[12-15]. The process of compression was quite different from the process of cervical spondylotic myelopathy presenting in the clinic[12-15].

This study used a novel spongy polyurethane material, which slowly absorbs water, expands and produces linear pressure. After saturation, its volume can remain stable over a long period of time, and the effect was close to the clinical onset characteristics. Moreover, this material is reproducible, and has good controllability and a high success rate[16]. Meanwhile, a posterior approach of the cervical vertebra was utilized in this

study, which implemented dorsal compression and avoided anterior approach-induced injury to important organs. Thus, the survival rate of models was greatly improved. The site of compression was $C_{5–6}$ that is commonly found in cervical spondylotic myelopathy, showing a perfect clinical correlation[17]. These strategies made simulated cervical spondylosis consistent with the clinical course, which is a precondition of studying neuropathological characteristics[6]. The persistence time of balloon dilatation and screw compression was controllable, but it should be operated repeatedly, which can cause acute spinal cord injury. Moreover, pressure changes are not linear, and the success rate of modeling is low[18]. Epidural implantation of tumor cells avoided acute and nonlinear compression, formed chronic compression on the spinal cord, but it could lead to local inflammatory reaction, systemic adverse reaction, short survival time and poor repeatability[19-20]. A previous study established a twy/twy rat model using transgenic technology[21]. This model could be induced to suffer from ligamentous ossification and thickening, which resulted in chronic spinal cord compression[21]. This model was consistent with clinical pathogenic mechanism, but its repeatability was poor, and the site of compression was not identical to that in the clinic[21]. In the models described above, objects for compression could induce acute spinal cord injury and/or severe inflammatory reaction, which was not consistent with clinical onset, and they were not the ideal animal model for chronic spinal cord compression injury[22].

The present study established an animal model of chronic cervical spondylotic myelopathy by implanting a novel spongy polyurethane material, and explored the histopathology of the injured spinal cord of rat models, and detected using MRI. This study sought to investigate the relationship of histopathological changes in the spinal cord to fractional anisotropy and average diffusion coefficient obtained by MRI.

RESULTS

Quantitative analysis of experimental animals

A total of 64 rats were equally and randomly assigned to sham surgery group (C_6 laminectomy) and model group (implantation of polyurethane film into $C_{3–5}$ epidural space after C_6 laminectomy to establish models of chronic cervical spondylotic myelopathy). Vital signs of rat models were closely observed. If death occurred before MRI and histological examination, the dead rats were replaced by new rat models. Five rats died during the experiment. A total of 64 rats were included in the final analysis.

Imaging alterations in the spinal cord of rat models of chronic cervical spondylotic myelopathy

The spinal cord was regular at 4, 24, 72 hours and 1 week after injury, and no abnormal high-signal-intensity area appeared in the sham surgery group.

In the model group, the implant did not expand at 4 hours after implantation. T1WI and T2WI and spectral presaturation with inversion recovery did not reveal abnormal high signal intensity or bleeding. At 24 hours after film implantation, the implant expanded and the spinal cord was obviously compressed. No abnormal signal intensity occurred in the compressed segment. At 72 hours, with expansion of the implant, the dorsal side of the spinal cord was noticeably compressed, but no bleeding or edema was visible. At 1 week, MRI revealed that the increase in implant volume was not obvious, but edema, hemorrhage and spinal cord softening were observed. Slightly high signal on T2WI was seen surrounding the implant.

Compared with the sham surgery group, the fractional anisotropy value reduced in the order of 4 hours < 24 hours < 72 hours < 1 week after implantation in the model group ($P < 0.01$ or $P < 0.05$; Table 1), but average diffusion coefficient significantly increased at 72 hours and 1 week after implantation ($P < 0.01$; Table 1).

Pathological changes in the compressed spinal cord of rat models of chronic cervical spondylotic myelopathy

As displayed in Figure 1, in the sham surgery group, hematoxylin-eosin staining demonstrated that no abnormal morphology was detected at 4, 24, 72 hours and 1 week after injury, and cells of the spinal gray matter also exhibited normal morphology. Luxol-fast-blue staining showed that the myelin sheath of white matter fiber was intact, regular and tight, with the presence of a lamellar structure; spinal cord structure was not damaged.

In the model group: at 4 hours after implantation, hematoxylin-eosin staining demonstrated that the spinal cord was slightly compressed; the spinal cord exhibited mild edema; nerve cells in the gray matter were slightly swollen; partial axons shrinkage had occurred; and the number of large motor neurons in the spinal anterior horn was reduced ($P < 0.01$). Furthermore, the intensity of Luxol-fast-blue staining began to decrease ($P < 0.01$).

Table 1 Changes in fractional anisotropy (FA) and average diffusion coefficient (ADC) in compressed spinal cord of rat models of chronic cervical spondylotic myelopathy (MRI scanning)

		Time after polyurethane film implantation			
		4 hours	24 hours	72 hours	1 week
FA	Sham surgery	0.73±0.03	0.72±0.06	0.72±0.03	0.73±0.06
	Model	0.68±0.03[a]	0.59±0.07[b]	0.51±0.12[b]	0.38±0.15[b]
ADC ($\times10^{-3}$ mm^2/s)	Sham surgery	1.23±0.05	1.21±0.07	1.22±0.08	1.23±0.07
	Model	1.26±0.03	1.23±0.11	1.65±0.12	1.71±0.15

[a]$P < 0.05$, [b]$P < 0.01$, *vs*. sham surgery group. Data are expressed as mean ± SD, with eight rats in each group at each time point. One-way analysis of variance and least significant difference test were used.

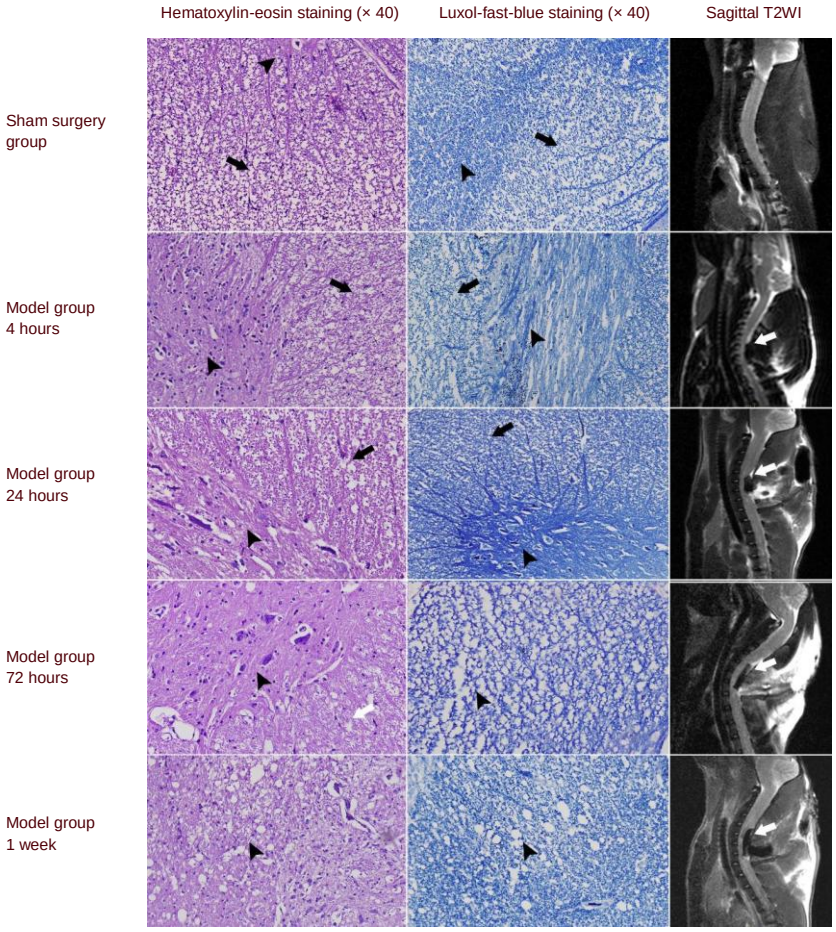

Figure 1 Histopathological changes and sagittal T2-weighted image (T2WI) in the compressed segment of the rat spinal cord.

In the sham surgery group, cell morphology was normal; white matter fibers were regularly arranged; and there was normal signal on T2WI.

In the model group, at 4 hours after implantation, hematoxylin-eosin staining demonstrated that the spinal cord was affected with mild edema; nerve cells in the gray matter were slightly swollen; and partial axons were shrunk. Luxol-fast-blue staining did not show obvious changes. There was normal signal on T2WI. At 24 hours, hematoxylin-eosin staining exhibited obvious edema; Luxol-fast-blue staining exhibited slightly disordered fiber bundles of the white matter and mild edema in axons; there was normal signal on T2WI. At 72 hours, hematoxylin-eosin staining revealed aggravated edema, disordered neuronal cells, some neuronal cell necrosis, as well as disordered and partially broken neurofilaments. Luxol-fast-blue staining demonstrated disordered white matter and twisted nerve fibers. There was normal signal on T2WI. At 1 week, hematoxylin-eosin staining showed spinal cord tissue loss and vacuolization, reduced number of large motor neurons, and reduced number of synapses. Luxol-fast-blue staining showed sparse decussating fibers in the gray matter and vacuole-like structure surrounding the axons; staining density of the myelin sheath decreased; and the thickness of the myelin sheath surrounding the axons became thin significantly. There was abnormal high signal on T2WI surrounding the implant.

In the images of hematoxylin-eosin staining, arrows show the anterior horn of the spinal cord; black arrowheads show the anterior funiculus of the spinal cord. In the images of Luxol-fast-blue staining, arrows show the posterior horn of the spinal cord; black arrowheads show the posterior funiculus of the spinal cord. On sagittal T2WI, white arrows show the implant.

Table 2 Comparison of the number of large motoneurons in the anterior horn and nerve fiber density of white matter in the compressed segment of the rat spinal cord

		Time after spinal cord injury			
		4 hours	24 hours	72 hours	1 week
Number of large motoneurons (cells/40-high power field)	Sham surgery	22.2±1.2	24.3±1.3	23.2±1.1	22.4±1.3
	Model	17.6±1.9[a]	14.8±1.3[a]	7.1±1.1[a]	2.7±0.8[a]
Nerve fiber density	Sham surgery	66.8±3.1	65.4±4.3	67.2±3.2	66.6±4.2
	Model	65.6±7.6	50.3±4.0[a]	23.8±7.2[a]	17.2±4.9[a]

The number of large motoneurons and Luxol-fast-blue staining intensity (representing nerve fiber density, no unit) gradually decreased in the model group, but no significant changes were detectable in the sham surgery group. [a]$P < 0.01$, *vs*. sham surgery group. Data are expressed as mean ± SD, with eight rats in each group at each time point. One-way analysis of variance and least significant difference test were used.

At 24 hours, hematoxylin-eosin staining revealed compressed spinal cord and obvious edema; and the number of large motor neurons in the spinal anterior horn was diminished ($P < 0.01$). Luxol-fast-blue staining exhibited slightly disordered fiber bundles in the white matter and mild edema in axons; and the staining intensity gradually decreased ($P < 0.01$). At 72 hours, hematoxylin-eosin staining revealed that the spinal cord was noticeably deformed; edema was further aggravated; neuronal cells were disordered; individual neuronal cell necrosis was visible and became spindle-shaped; neurofilaments were disordered and partially broken; and the number of large motor neurons in the anterior horn was further reduced ($P < 0.01$). Luxol-fast-blue staining demonstrated that the posterior horn of spinal gray matter became narrow and long; the posterior funiculus and lateral funiculus of white matter were disordered; nerve fibers were twisted and broken; and the staining intensity was diminished ($P < 0.01$). At 1 week, hematoxylin-eosin staining showed that the spinal cord was obviously deformed; tissue loss and vacuolization were observed; the number of large motor neurons in the anterior horn was reduced; the cytoplasm was reduced, karyolysis had occurred and there was a reduction in the number of synapses ($P < 0.01$); and cell number was decreased to the lowest value ($P < 0.01$). Luxol-fast-blue staining showed that decussating fibers in the gray matter were sparse; vacuole-like structures were observed surrounding the axons; the staining density of the myelin sheath was decreased ($P < 0.01$); the thickness of the myelin sheath surrounding the axons became significantly thinner, and the staining intensity was lowest ($P < 0.01$). The counting of large motor neurons in the anterior horn and Luxol-fast-blue staining intensity were shown in Table 2.

DISCUSSION

At 4 to 24 hours after implantation, the rat spinal cord had mild edema, venous congestion and an expanded central canal from the beginning of compression to the largest expansion of the material. MRI did not reveal epidural and subdural space or intramedullary hemorrhage, which suggests that the pathological process of this compression did not begin from acute spinal cord injury[23]. At 72 hours after implantation, nerve fiber structure was disordered and neurofilaments were broken, which could be induced by persistent compression, venous congestion and severe edema. At 1 week after implantation, vacuoles formed, the number of neurons began to decrease, and neuronal tracts were demyelinated. At this time, neurological function of rats was mildly disturbed, which was possibly associated with ischemia in the compressed tissues[24]. Above mentioned pathological changes were identical to that in the early stage of cervical spondylotic myelopathy[25]. Cervical spondylotic myelopathy is a spinal nerve dysfunction induced by chronic progressive spinal compression, and its corresponding pathological alterations contain venous congestion, tiny intramedullary focal necrotic site, cystic cavities, Wallerian degeneration in the nerve tracts of the posterior and lateral funiculi, fibroglial scar formation, and motor neuron death in the anterior horn[26]. In this study, MRI, with gross specimen and pathological morphological examination confirmed that the posterolateral spinal cord was deformed, but there was no intramedullary hemorrhage, histiocyte necrosis, inflammatory cell infiltration, or acute neurological functional loss. With the expansion of the material, the spinal cord suffered from a progressive compression, which was consistent with the early pathological characteristics of chronic spinal cord compression injury. Thus, it provides a reliable model and theory basis for the studying the pathomechanism and early intervention of cervical spondylotic myelopathy.

Previous studies have investigated similar approaches using 11T MRI and confirmed that research-oriented MRI could be used to obtain images with high resolution and excellent signal-to-noise ratio[27]. In this study, we utilized 1.5T MRI. Clinically-oriented MRI has a certain technical

challenge for cervical cord scanning in rats.

This study used a 47 mm coil, which could obtain high resolution. Simultaneously, 35 gradient directions were scanned, which greatly elevated signal-to-noise ratio. Based on the two advantages described above, diffusion tensor imaging utilized a high *b* value and long repetition time, so these optimal parameters ensured image quality and data accuracy[1, 7, 12]. Therefore, clinically-oriented MRI could also be used to successfully conduct rat experiments. Moreover, clinical cases were also diagnosed by clinically-oriented MRI. However, clinically-oriented MRI has some disadvantages in rat models. For example, the cervical cord of rats could not be divided into the anterior funiculus and posterior funiculus using clinically-oriented MRI. That is to say, its resolution was not high enough compared with research-oriented MRI. Nevertheless, results verified that the data obtained from clinically-oriented MRI provided reliable evidence for studying the correlation of diffusion tensor imaging and pathological alterations.

White matter fibers were tightly arranged in normal cervical cord. Due to the myelin sheath barrier, the diffusion tendency of hydrone in white matter myelin sheath was less in the direction of vertical to white matter fiber distribution than that in the direction of identical to white matter fiber distribution, showing a high fractional anisotropy. In the model group, at 4 hours after implantation, the alteration in the space between the axon and myelin sheath had great effects on the diffusion of hydrone among fiber tracts due to axonal injury. Fractional anisotropy represents the sum of diffusion tendency of hydrone in various directions[28]. When the fractional anisotropy value was abnormal and average diffusion coefficient was not altered, the cervical cord would be in an early stage of compression. At this time, axons shrunk and the myelin sheath was intact[29-30]. At 24 hours after implantation, edema became obvious and Luxol-fast-blue staining decreased, indicating that partial fibers were demyelinated[31]. Average diffusion coefficient increased in some rats, but no significant difference in average diffusion coefficient was detected compared with the sham surgery group. Average diffusion coefficient alteration appears after demyelination to a certain extent, so people should be cautious about using average diffusion coefficient to diagnose pathological changes in demyelination[32-33]. Hematoxylin-eosin staining revealed wide axonal atrophy; simultaneously, fractional anisotropy value noticeably decreased. From 4 to 24 hours after implantation, regarding the pathological changes in axons with cervical cord compression injury, the sensitivity of fractional anisotropy value was higher than that of average diffusion coefficient. Fractional anisotropy could reflect the pathological changes of early cervical cord injury. At 72 hours after implantation, hematoxylin-eosin staining and Luxol-fast-blue staining demonstrated that vacuoles appeared, the number of neurons were significantly reduced, and nerve tracts were extensively demyelinated[34-36]. As the spinal cord was compressed for a long time and ischemia had occurred, the neurological function of rats experienced mild impairment[34-36]. Fractional anisotropy and average diffusion coefficient also diminished as compared with those at 4, 24 and 72 hours after implantation, which could be a result of glial scar formation and Wallerian degeneration[37-39]. Conventional T2WI exhibited high signals on the site of compression.

In summary, from 4 to 24 hours after implantation, fractional anisotropy values decreased due to pathological changes in axons. Average diffusion coefficient was normal, because the fiber bundle myelin sheath of the cervical cord was intact. From 24 to 72 hours, the fractional anisotropy value reduced and the average diffusion coefficient increased, because axonal injury and demyelination existed at the same time[40-42]. With persistent compression, extensive vacuolization, severe axonal injury and demyelination appeared at 1 week. The fractional anisotropy value obviously decreased, but average diffusion coefficient significantly increased. Simultaneously, conventional T2WI revealed high signals at the site of compression. Diffusion tensor imaging can simultaneously measure the average diffusion coefficient and fractional anisotropy value, even three-dimensional fiber bundle tracking[43]. Results confirmed that combined average diffusion coefficient and fractional anisotropy value can provide an early diagnosis for cervical cord compression, evaluate pathological changes, and provide useful references for the prevention and treatment of chronic cervical spondylotic myelopathy.

MATERIALS AND METHODS

Materials

Healthy 8-week-old Sprague-Dawley rats weighing 350–450 g (30 males and 34 females) were purchased from Guangdong Provincial Medical Experimental Animal Center in China, Animal License No. SCXK (Yue) 2008-0002. The protocols were conducted in accordance with the *Guidance Suggestions for the Care and Use of Laboratory Animals*, formulated by Ministry of Science and Tech-

nology of China[44].

Methods

Establishment of rat models of chronic cervical spondylotic myelopathy

All rats were intraperitoneally anesthetized with 10% chloral hydrate (1 mL/kg). In accordance with previously published method[45], the $C_{5–6}$ intervertebral space was exposed under a light microscope (BX51, Olympus, Tokyo, Japan). After the ligament flava was removed and the spinal dura mater was separated, 2.5 mm × 5.0 mm × 0.8 mm polyurethane film (coprepared with Research Room of Orthopedic Surgery, The University of Hong Kong, China) was implanted in the space between the $C_{5–6}$ vertebral plate and spinal dura mater in the model group. After hemostasis, the incision was sutured. Spinal cord injury and cerebrospinal fluid leakage should be avoided during the operation. After implantation, all rats were intramuscularly injected with penicillin to prevent infection.

After mode induction, the rats were fed in separate cages, and allowed free access to food and activity. The model was successfully established if the polyurethane film compressed the cervical cord in the cervical spinal canal, as verified by MRI scanning.

MRI of rat spinal cord

The rats of the two groups underwent Philips Achieva Dual HP 1.5 T MRI scanner (Philips Medical Systems Nerderland B.V. Veenpluis 4-6, 5684 PC Best, the Netherlands), with a 47 mm coil, at 4, 24, 72 hours and 1 week after implantation to observe the spinal cord cervical segments. Sagittal images at the $C_{5–6}$ level were obtained by conventional scanning. T1WI: repetition time/echo time = 500 ms/22 ms; T2WI: repetition time/echo time = 3 000 ms/90 ms, turbo spin-echo sequence was used. Some rats underwent sagittal and/or coronal scanning; thickness 2 mm, interval 0.1 mm, resolution 0.27 mm × 0.27 mm × 2.0 mm. Epidural space and intramedullary hemorrhage, edema and softening were observed. Using single shot plane echo spin echo-echo planar imaging sequence and sagittal diffusion tensor imaging, field of view 65 mm × 50 mm × 38 mm, resolution 1 mm × 1.3 mm × 1.5 mm, repetition time/echo time = 8 100 ms/ 93 ms, flip angle 90°, five slices, interval 0 mm, diffusion gradient direction 35, *b* value 800 s/mm^2, collection twice, fat-suppression technique: spectral presaturation with inversion recovery, automated shimming, imaging time: 7 minutes, 20 seconds. Using diffusion tensor imaging software package, in the model group, the image of compressed cervical cord was selected; cross section of cervical cord was considered as region of interest; fractional anisotropy value was directly read. The sham surgery group was measured by the same method described above.

Average diffusion coefficient values of rats in both groups were measured using the average diffusion coefficient measure tool of diffusion tensor imaging software package. T2 signal in the region of interest was evaluated by two associate chief physicians using the double blind method. Signal difference was calculated by (signal intensity in the site of compression – signal intensity in the site of non-compression)/signal intensity in the site of non-compression. Signal difference ≥ 25% represents signal abnormality[45].

Pathology of rat spinal cord undergoing compression

The rats were overanesthetized with sodium pentobarbital (40 mg/kg) immediately after MRI scanning, causing death. The rats were injected with 50 mL heparin-saline *via* ascending aorta, and fixed with 300 mL formaldehyde trinitrophenol solution (4% formaldehyde and 0.4% trinitrophenol in 0.16 mol/L phosphate buffer, pH 7.4). The cervical vertebra was immersed in 4% phosphate-buffered formaldehyde for 3 days. The spinal cord was isolated and stored in 4% phosphate-buffered formaldehyde for 48 hours, followed by paraffin imbedding. The spinal cord at $C_{5–6}$ and its surrounding segments were sliced into 8 μm-thick series sections. The sections underwent hematoxylin-eosin staining and Luxol-fast-blue staining. Hematoxylin-eosin staining was used to observe the number, morphology, and distribution of spinal anterior horn neurons, intramedullary hemorrhage, edema, degeneration, necrosis, and inflammatory cell infiltration. Luxol-fast-blue staining was utilized to observe arrangement and demyelination of nerve tracts of the spinal white matter. Light staining represented low density of white matter nerve fibers, indicating severe demyelination.

Using Image-Pro Plus 6.0 image analysis software (Media Cybernetics Inc., Rockville, MD, USA), five high-power fields (40 ×) were randomly selected in the spinal anterior horn. Large motoneurons were quantified and the average was calculated. In the images of Luxol-fast-blue staining, five high-power fields (40 ×) were randomly selected in the white matter of compressed segment of spinal cord. The absorbance values were detected, and their average was calculated.

Statistical analysis

Measurement data were expressed as mean ± SD, and analyzed with SPSS 17.0 software (SPSS, Chicago, IL, USA). Comparisons among multiple groups were performed using one-way analysis of variance. Paired intergroup comparisons were conducted using the least significant difference test. A value of $P < 0.05$ was considered statistically significant.

REFERENCES

[1] Smith SA, Jones CK, Gifford A, et al. Reproducibility of tract-specific magnetization transfer and diffusion tensor imaging in the cervical spinal cord at 3 tesla. NMR Biomed. 2010;23(2):207-217.

[2] Mulcahey M, Samdani A, Gaughan J, et al. Diffusion tensor imaging in pediatric spinal cord injury: preliminary examination of reliability and clinical correlation. Spine. 2012;37(13):E797-803.

[3] Hori M, Fukunaga I, Masutani Y, et al. New diffusion metrics for spondylotic myelopathy at an early clinical stage. Eur Radiol. 2012;22(8):1797-1802.

[4] Hu Y, Wen CY, Li TH, et al. Somatosensory-evoked potentials as an indicator for the extent of ultrastructural damage of the spinal cord after chronic compressive injuries in a rat model. Clin Neurophysiol. 2011;122(7):1440-1447.

[5] Lonjon N, Kouyoumdjian P, Prieto M, et al. Early functional outcomes and histological analysis after spinal cord compression injury in rats. J Neurosurg Spine. 2010;12(1):106-113.

[6] Kim TH, Zollinger L, Shi XF, et al. Quantification of diffusivities of the human cervical spinal cord using a 2D single-shot interleaved multisection inner volume diffusion-weighted echo-planar imaging technique. AJNR Am J Neuroradiol. 2010;31(4):682-687.

[7] Kim JH, Song SK, Burke DA, et al. Comprehensive locomotor outcomes correlate to hyperacute diffusion tensor measures after spinal cord injury in the adult rat. Exp Neurol. 2012;235(1):188-196.

[8] Kim JH, Loy DN, Wang Q, et al. Diffusion tensor imaging at 3 hours after traumatic spinal cord injury predicts long-term locomotor recovery. J Neurotrauma. 2010;27(3):587-598.

[9] Andre J B, Bammer R. Advanced diffusion-weighted magnetic resonance imaging techniques of the human spinal cord. Top Magn Reson Imaging. 2010;21(6):367-378.

[10] Buchy L, Luck D, Czechowska Y, et al. Diffusion tensor imaging tractography of the fornix and belief confidence in first-episode psychosis. Schizophr Res. 2012;137(1-3):80-84.

[11] Cheran S, Shanmuganathan K, Zhuo J, et al. Correlation of MR diffusion tensor imaging parameters with ASIA motor scores in hemorrhagic and nonhemorrhagic acute spinal cord injury. J Neurotrauma. 2011;28(9):1881-1892.

[12] Kamble RB, Venkataramana NK, Naik AL, et al. Diffusion tensor imaging in spinal cord injury. Indian J Radiol Imaging. 2011;21(3):221-224.

[13] Cui JL, Wen CY, Hu Y, Orientation entropy analysis of diffusion tensor in healthy and myelopathic spinal cord. Neuroimage. 2011;58(4):1028-1033.

[14] Petersen JA, Wilm BJ, von Meyenburg J, et al. Chronic cervical spinal cord injury: DTI correlates with clinical and electrophysiological measures. J Neurotrauma. 2012;29(8):1556-1566.

[15] Théaudin M, Saliou G, Denier C, et al. A Correlation between fractional anisotropy variations and clinical recovery in spinal cord infarctions. J Neuroimaging. 2013;23(2):256-258.

[16] Barakat N, Mohamed FB, Hunter LN, et al. Diffusion tensor imaging of the normal pediatric spinal cord using an inner field of view echo-planar imaging sequence. AJNR Am J Neuroradiol. 2012;33(6):1127-1133.

[17] Lundell H, Barthelemy D, Biering-Sørensen F, et al. Fast diffusion tensor imaging and tractography of the whole cervical spinal cord using point spread function corrected echo planar imaging. Magn Reson Med. 2013;69(1):144-149.

[18] Freund P, Wheeler-Kingshott CA, Axonal integrity predicts cortical reorganisation following cervical injury. J Neurol Neurosurg Psychiatry. 2012;83(6):629-637.

[19] Sąsiadek MJ, Szewczyk P, Bladowska J. Application of diffusion tensor imaging (DTI) in pathological changes of the spinal cord. Med Sci Monit. 2012;18(6):73-79.

[20] Zhang J, Aggarwal M, Mori S. Structural insights into the rodent CNS via diffusion tensor imaging. Trends Neurosci. 2012;35(7):412-421.

[21] Jones JG, Cen SY, Lebel RM, et al. Diffusion tensor imaging correlates with the clinical assessment of disease severity in cervical spondylotic myelopathy and predicts outcome following surgery. AJNR Am J Neuroradiol. 2013;34(2):471-478.

[22] Rajasekaran S, Kanna RM, Shetty AP. Diffusion tensor imaging of the spinal cord and its clinical applications. J Bone Joint Surg Br. 2012;94(8):1024-1031.

[23] Wang W, Qin W, Hao N, et al. Diffusion tensor imaging in spinal cord compression. Acta Radiol. 2012;53(8):921-928.

[24] Uda T, Takami T, Tsuyuguchi N, et al. Assessment of cervical spondylotic myelopathy using diffusion tensor magnetic resonanceimaging parameter at 3.0 tesla. Spine. 2013;38(5):407-414.

[25] Yang AW, Jensen JH, Hu CC, et al. Effect of cerebral spinal fluid suppression for diffusional kurtosis imaging. J Magn Reson Imaging. 2013;37(2):365-371.

[26] Smith SA, Pekar JJ, Van Zijl PC. Advanced MRI strategies for assessing spinal cord injury. Handb Clin Neurol. 2012;109:85-101.

[27] Pieper CC, Konrad C, Sommer J, et al. Structural changes

of central white matter tracts in Kennedy's disease - a diffusion tensor imaging and voxel-based morphometry study. Acta Neurol Scand. 2013;127(5):323-328.

[28] Gasparotti R, Lodoli G, Meoded A, et al. Feasibility of diffusion tensor tractography of brachial plexus injuries at 1.5 T. Invest Radiol. 2013;48(2):104-112.

[29] Mohammadi S, Freund P, Feiweier T, et al. The impact of post-processing on spinal cord diffusion tensor imaging. Neuroimage. 2013;15(70):377-385.

[30] Griffin JF 4th, Cohen ND, Young BD, et al.Thoracic and lumbar spinal cord diffusion tensor imaging in dogs. J Magn Reson Imaging. 2013;37(3):632-641.

[31] Konomi T, Fujiyoshi K, Hikishima K, et al. Conditions for quantitative evaluation of injured spinal cord by in vivo diffusion tensor imagingand tractography: preclinical longitudinal study in common marmosets. Neuroimage. 2012;63(4):1841-1853.

[32] Bazley FA, Pourmorteza A, Gupta S, et al. DTI for assessing axonal integrity after contusive spinal cord injury and transplantation of oligodendrocyte progenitor cells. Conf Proc IEEE Eng Med Biol Soc. 2012;2012:82-85.

[33] Hutchinson EB, Sobakin AS, Meyerand ME, et al. Diffusion tensor MRI of spinal decompression sickness. Undersea Hyperb Med. 2013;40(1):23-31.

[34] Lee JW, Kim JH, Park JB, Diffusion tensor imaging and fiber tractography in cervical compressive myelopathy: preliminary results. Skeletal Radiol. 2011;40(12):1543-1551.

[35] Nakamura M, Fujiyoshi K, Tsuji O, et al. Clinical significance of diffusion tensor tractography as a predictor of functional recovery after laminoplasty in patients with cervical compressive myelopathy. J Neurosurg Spine. 2012; 17(2):147-152.

[36] Pease A, Miller R. The use of diffusion tensor imaging to evaluate the spinal cord in normal and abnormal dogs. Vet Radiol Ultrasound. 2011;52(5):492-497.

[37] Hansen B, Flint JJ, Heon-Lee C, et al. Diffusion tensor microscopy in human nervous tissue with quantitative correlation based on direct histological comparison. Neuroimage. 2011;57(4):1458-1465.

[38] Kim JH, Song SK. Diffusion tensor imaging of the mouse brainstem and cervical spinal cord. Nat Protoc. 2013;8(2): 409-417.

[39] Padhani AR, van Ree K, Collins DJ, et al. Assessing the relation between bone marrow signal intensity and apparent diffusion coefficient in diffusion-weighted MRI. AJR Am J Roentgenol. 2013;200(1):163-170.

[40] Robertson RL, Maier SE, Mulkern RV, et al. MR line-scan diffusion imaging of the spinal cord in children. AJNR Am J Neuroradiol. 2007;21(7):1344 -1348.

[41] Chou MC, Lin YR, Huang TY, et al. FLAIR diffusion-tensor MR tractography comparison of fiber tracking with conventional imaging. AJNR Am J Neuroradiol. 2005;26(3): 591-597.

[42] Carballido-Gamio J, Xu D, Newitt D, et al. Single-shot fast spin-echo diffusion tensor imaging of the lumbar spine at 1.5 and 3 T. Magn Reson Imaging. 2007;25(5):665-670.

[43] Summers P, Staempfli P, Jaermann T, et al. A preliminary study of the effects of trigger timing on diffusion tensor imaging of the human spinal cord. AJNR Am J Neuroradiol. 2006;27(9):1952-1961.

[44] The Ministry of Science and Technology of the People's Republic of China. Guidance Suggestions for the Care and Use of Laboratory Animals. 2006-09-30.

[45] Facon D, Ozanne A, Fillard P, et al. MR diffusion tensor imaging and fiber tracking in spinal cord compression. AJNR Am J Neuroradiol. 2005;26(6):1587-1594.

(Reviewed by Wallace M, Robens J, Sun XJ, Sun HR)
(Edited by Wang J, Qiu Y, Li CH, Song LP, Liu WJ, Zhao M)